# Assessing protective interventions on cholera dynamics using a Caputo-Fabrizio fractional model.

Received: April 2025
Revised: July 2025
Accepted: 18 July 2025

[1]Joseph Adeleke Adedeji, [1]Morufu Oyedunsi Olayiwola,

[1]Department of Mathematical Sciences, Osun State University, Osogbo, Nigeria.

Email: joseph.adedeji@uniosun.edu.ng;olayiwola.oyedunsi@uniosun.edu.ng

**Abstract:** This study introduces a mathematical framework that incorporates fractional-order derivatives to investigate how effective protective interventions are in high-risk cholera populations. The model establishes disease-free and endemic thresholds, with stability analyzed using the Routh-Hurwitz criteria. A key insight is that determining the basic reproduction number provides deeper understanding of cholera transmission dynamics.

Through normalized sensitivity analysis, the ingestion rate of Vibrio cholerae emerges as the most influential factor in transmission. Meanwhile, vaccination coverage and awareness of protective measures are recognized as crucial elements for cholera control and eradication.

The model uses the Caputo-Fabrizio fractional-order approach and is proven to be well-posed through the fixed-point theorem. Using the Laplace Adomian Decomposition Method (LADM), the results demonstrate that high vaccination rates and widespread adoption of protective measures among susceptible individuals in high-risk zones significantly reduce susceptibility, increase protected populations, and strengthen overall public health resilience against cholera.

***Keywords:*** *LADM, Stability Analysis, vaccination and awareness, numerical experiments, basic reproduction number, novel mathematical model.*

## 1. INTRODUCTION

Cholera, caused by Vibrio cholerae, remains a significant global health threat, spreading through contaminated water and food sources and causing severe diarrhea, vomiting, and dehydration that can be fatal without prompt treatment [1-3]. Outbreaks predominantly occur in regions with poor sanitation and limited clean water access [4], with rural riverine communities being particularly vulnerable high-risk areas where cases continue to surge despite eradication efforts. Mathematical modeling has become instrumental in understanding cholera transmission dynamics, with studies identifying key risk factors and demonstrating the effectiveness of vaccination strategies [5] and prevention measures [6-10]. Recent advances in fractional calculus have enhanced disease modeling capabilities, with fractional-order operators like Riemann-Liouville [11], Caputo [12-15], and Caputo-Fabrizio [16,17] proving valuable for capturing complex transmission dynamics, as demonstrated by Baba et al.'s [18] fractional-order cholera model, Helikumi et al.'s [19] transmission model, and Rosa and Torres' [20] optimal control strategies. This study aims to analyze and evaluate the role of protective intervention measures, specifically educational programs and vaccinations, in cholera transmission control within high-risk riverine communities by presenting a novel seven-compartment deterministic mathematical model that incorporates protective interventions to assess their effectiveness in reducing cholera transmission dynamics in vulnerable populations.

### 1.1. Preliminary Concepts

This section provides essential definitions of fractional calculus that are relevant to the current study.

**Definition 1:** Let $W \in K^{1}[0,B], B>0, \rho \in (0,1)$, the CF fractional derivative operator is given by

$$^{CF}D_t^{\rho}(W(t)) = \frac{N(\rho)}{1-\rho}\int W'(\delta)e^{-\left[\rho\frac{\tau-v}{1-\rho}\right]}d\delta$$

where $N(\rho)=N(0)=1$ is a normalize function.

**Definition 2:** The CF integral of function $W(t)$ withorder $0<\rho<1$ is

$$^{CF}I_t^{\rho}[W(t)] = \frac{2(1-\rho)}{(1-\rho)N(\rho)}W(t)+\frac{2\rho}{(2-\rho)N(\rho)}\int_0^t W(\delta)d\delta,\ t\geq 0$$

**Definition 3:**
The Laplace transform of CF derivative of order $\rho \in (0,1)$, is: $L\left[{}^{CF}D_t^{\rho}W(t)\right] = \frac{sL[r(t)]-g(0)}{s+q(1-s)}$ $s\geq 0$

**Definition 4:**

The Adomian polynomials $B_0, B_{1,\ldots} B_n$ used to decompose unknown function $r(t)$ is given by $r(t) = r_0 + r_1 + r_2 + r_n$ is: $B_n = \frac{1}{m}\frac{d^m}{d\lambda^m}\left[ H(t)\sum_{j=0}^{m} r_j \lambda^j \right]_{\lambda=0}$

## 2. METHODOLOGY

### 2.1. Laplace-Adomian decomposition Method (LADM)

This subsection outlines the LADM method for solving a generalised fractional order differential equation given by:

$$ {}_t^{CF}D^{\eta}\Psi_j(t) = \begin{bmatrix} l_j(\Psi_1, \Psi_2, \Psi_3, \Psi_j) + \\ n_i(\Psi_1, \Psi_2, \Psi_3, \Psi_j) \end{bmatrix} \quad (1)$$

Subject to:

$\Psi_j^{u_i}(0) = \varpi_u^j$ ,for , $j = 1,2,3\ldots r$ and $k_{j-1} \le \rho \le k_j$

In (1), ${}_t^{CF}D^{\rho}\Psi_j(t)$ represents CF operator of $j$ numbers of unknown functions $\Psi(t)$. The linear and nonlinear terms are represented by $l_j$ & $m_j$ . Taking the Laplace transform of (1),

$$ L\left[ {}_t^{CF}D^{\rho}\Psi_j(t) \right] = L\begin{bmatrix} l_j(\Psi_1, \Psi_2, \Psi_3, \Psi_j) \\ +m_J(\Psi_1, \Psi_2, \Psi_3, \Psi_j) \end{bmatrix} \quad (2)$$

Imposing Definition 2 on (3),

$$ \frac{vL\left[\Psi_j(t)\right] - \Psi_j(0)}{v + \rho(1-\rho)} = L\begin{bmatrix} l_j(\Psi_1, \Psi_2, \Psi_3, \Psi_j) \\ +m_j(\Psi_1, \Psi_2, \Psi_3, \Psi_j) \end{bmatrix} \quad (3)$$

By Definition (4), $W_j(t)$ can be decomposed as,

$$ \Psi_j(t) = \sum_{s=0}^{\infty} \Psi_{js}(t) \quad s = 1,2,\ldots n \quad (4)$$

Nonlinear terms are given by,

$$ m_j(\Psi_1, \ldots \Psi_j) = \sum_{s=0}^{\infty} B_{ji}(t) \;\; i = 1,2,\ldots n \quad (5)$$

Where $B_{ij}$ is the Adomian polynomial. Evaluating (3) with (4) and (5) yields

$$ L\left[\sum_{j=0}^{\infty} r_{ij}(t)\right] = \frac{r_i^{k_i}(0)}{s} + \frac{s+\alpha(1-s)}{s}\begin{pmatrix} L\left[ L_i\left( \sum_{j=0}^{\infty} r_{1j}(t), \ldots, \sum_{j=0}^{\infty} r_{mj}(t) \right) \right] \\ +L\left[ \sum_{j=0}^{\infty} B_{ij}(t) \right] \end{pmatrix} \quad (6)$$

The inverse Laplace transform of (6) yields $r_{1j}, r_{2j}, r_{n,j}, j \ge 0$ and simplification of the preceding equation yields

$$ r_{i(j+1)}(t) = c_k^i + L^{-1}\begin{pmatrix} \frac{s+\alpha(1-s)}{s} L\left[ L_i\left( \sum_{j=0}^{\infty} r_{1j}(t), \ldots, \sum_{j=0}^{\infty} r_{mj}(t) \right) \right] \\ +L\left[ \sum_{j=0}^{\infty} B_{ij}(t) \right] \end{pmatrix} $$

Which is the required recurrence relation.

### 2.2. Model Formulation

We categorised the population at time $t$ into susceptible $S(t)$, vaccinated $V(t)$, protected $P(t)$, infected $I(t)$, hospitalised $H(t)$, and recovered $R(t)$. $B(t)$ Represents vibrio cholera concentration.

$$ \left.\begin{aligned} \frac{dS}{dt} &= \Lambda - (\beta_c\lambda + \beta_h I + \mu + \phi + \eta)S + \varepsilon R, \\ \frac{dV}{dt} &= \phi S - (\sigma + \mu)V, \\ \frac{dP}{dt} &= AS(\beta_c\lambda + \beta_h I) + \eta S - \mu P, \\ \frac{dI}{dt} &= (\beta_c\lambda + \beta_h I)(1-A)S - (\gamma_1 + \gamma_2 + d_1 + \mu)I, \\ \frac{dH}{dt} &= \gamma_1 I - (\tau + d_2 + \mu)H, \\ \frac{dR}{dt} &= \sigma V + \tau H + \gamma_2 I - \varepsilon R - \mu R, \\ \frac{dB}{dt} &= \theta I - \delta B. \end{aligned}\right\} \quad (7)$$

The susceptible population $S(t)$ increases through birth rate $\Lambda$ and relapse from recovered individuals $\varepsilon$, while decreasing due to natural mortality $\mu S$, vaccination rate of susceptible $\phi S$, protection through awareness $\eta S$, and force of infection $(\beta_c\lambda + \beta_h I)S$ at infected individuals $\beta_h I$ and the rate at which people ingest vibrio cholera particles $\beta_c\lambda$. The vaccinated population $V(t)$ increases through vaccination of susceptible $\phi S$ and decreases due to natural mortality $\mu V$ and vaccine-induced recovery $\sigma V$. The protected population $P(t)$ increases through direct protection of susceptible $\eta S$ and awareness-based protection during exposure $AS(\beta_c\lambda + \beta_h I)$, while decreasing due to natural mortality $\mu P$. The infected population $I(t)$ increases through infection of unprotected susceptible $(1-A)S(\beta_c\lambda + \beta_h I)$ and decreases due to natural mortality $\mu I$, hospitalization $\gamma_1 I$, natural recovery $\gamma_2 I$, and disease-induced mortality $d_1 I$. The hospitalized population $H(t)$ increases through hospitalization from

infected $\gamma_1 I$ and decreases due to natural mortality $\mu H$, treatment recovery $\tau H$, and disease-induced mortality $d_2 H$. The recovered population $R(t)$ increases through recovery from vaccination $\sigma V$, hospitalization $\tau H$, and natural recovery from infection $\gamma_2 I$, while decreasing due to natural mortality $\mu R$ and relapse rate $\varepsilon R$. The vibrio cholerae concentration $B(t)$ increases through bacterial shedding from infected individuals $\theta I$ and decreases through natural decay $\delta B$. Additionally, across all population groups, there exists a natural mortality rate $\mu$. Equation (7) form the proposed mathematical model of cholera disease. The nomenclature of model's component are itemised in Table 1. Subject to:

$$S_0(t) = m_1,\ V_0(t) = m_2,\ P_0(t) = m_3,\ I_0(t) = m_4,$$
$$H_0(t) = m_5, R_0(t) = m_6,\ B_0(t) = m_7.$$

For simplicity of model terms, let

$$a_0 = \varepsilon\delta\phi, a_1 = (\mu + \phi + \eta),\ a_2 = (\sigma + \mu)$$
$$a_3 = (\gamma_1 + \gamma_2 + d_1 + \mu),\ a_4 = (\tau + d_2 + \mu),$$
$$a_5 = (\varepsilon + \mu),\ a_6 = (\mu + \phi\eta)\ a_7 = a_6 + a_5 + a_2 + a_0.$$

**Table 1:** Variables, Parameters and their respective values

| **Variables** | **Description** |
|---|---|
| $S(t)$ | Time count of susceptible population |
| $V(t)$ | Time count of vaccinated population |
| $P(t)$ | Time count of protected population |
| $I(t)$ | Time count of infected population |
| $H(t)$ | Time count of hospitalised population |
| $R(t)$ | Time count of recovered population |
| $B(t)$ | Time concentration of vibrio cholera density |
| **Parameters** | Description |
| $\Lambda$ | Recruitment rate |
| $\beta_c$ | Human-to-human transmission rate |
| $\beta_h$ | Vibrio ingestion rate from the environment |
| $\lambda$ | Force of infection |
| $A$ | Adoption rate of protective measures of high risk individuals |
| $\mu$ | Mortality rate |
| $\phi$ | Vaccination rate among the susceptible population |
| $\eta$ | Progression rate of susceptible population |
| $\varepsilon$ | Relapse rate |
| $\sigma$ | Recovery rate among the vaccinated |
| $\gamma_1$ | Hospitalisation rate for infected individuals |
| $\gamma_2$ | Natural recovery rate |
| $d_1$ | Infection-induced mortality rate among the infected |
| $\tau$ | Treatment rate |
| $d_2$ | Infection-induced mortality rate among the hospitalised |
| $\delta$ | Death rate of vibrio cholera |
| $\theta$ | Influx rate of vibrio cholera |

### 2.3. Cholera Model Analysis

In this section, we compute the two critical points of (7). This include calculating the disease free equilibrium and endemic equilibrium points.

#### 2.3.1. Disease Free Equilibria

At this critical point, (7) is devoid of disease. That is, there is zero concentration of vibrio cholera population and there is no infected or hospitalised individual. Thus, $I = H = B = 0$, and the disease free equilibrium is,

$$\left.\begin{aligned} S_0 &= \frac{\Lambda a_2 a_5}{a_7},\ V_0 = \frac{\varphi\Lambda a_5}{a_7},\ P_0 = \frac{\eta\Lambda a_2 a_5}{\mu a_7}, \\ I_0 &= 0,\ H_0 = 0,\ R_0 = \frac{\sigma\varphi\Lambda}{a_7},\ B_0 = 0. \end{aligned}\right\} \quad (8)$$

#### 2.3.2. Endemic Equilibrium

At this phase of critical point, (7) contains the infected and bacterial population. Thus, $I \neq 0, H \neq 0, B \neq 0$.

$$S^* = \frac{\Lambda a_2 a_4 a_5 + \varepsilon\tau\gamma_1 I^* a_2 + \varepsilon\gamma_2 I^* a_2 a_4}{\left(\beta_c\lambda + \beta_h I^* + a_2 - \varepsilon\delta\phi a_4\right)},$$
$$V^* = \frac{\phi S^*}{a_2}, P^* = \frac{S^* A\left(\beta_c\lambda + \beta_h I^* + \eta\right)}{\mu},$$
$$I^* = \frac{\beta_c\lambda(1-A)S^*}{a_3 - \beta_h S^*(1-A)}, H^* = \frac{\gamma_1 I^*}{a_4}, \quad (9)$$
$$R^* = \frac{\sigma\phi S^* a_4 + \tau\gamma_1 I^* a_2 + \gamma_2 I^* a_2 a_4}{a_2 a_4 a_5}, \; B^* = \frac{\theta I^*}{\delta}$$

### 2.3.3. Linear Stability of Disease Free Equilibrium

The local stability of the disease-free equilibrium point is proven here using the following theorem.

**Theorem 1:** The critical point corresponding to the disease-free state of (7) is asymptotically stable if the real parts of all roots of the characteristic (10) are negative.

**Proof:** To prove this, consider the Jacobian matrix of (10) corresponding to (7) given by

$$J = \begin{bmatrix} -(\beta_c\lambda + a_1) & \varphi & A\beta_c\lambda + \eta & \beta_c\lambda(1-A) & 0 & 0 & 0 \\ 0 & -a_2 & 0 & 0 & 0 & \sigma & 0 \\ 0 & 0 & -\mu & 0 & 0 & 0 & 0 \\ \frac{-\Lambda\beta_h a_2 a_5}{a_7} & 0 & \frac{\Lambda A\beta_h a_2 a_5}{a_7} & \frac{\beta_h\Lambda a_2 a_5(1-A) - a_7 a_3}{a_7} & \gamma_1 & \gamma_2 & \theta \\ 0 & 0 & 0 & 0 & -a_4 & \tau & 0 \\ \varepsilon & 0 & 0 & 0 & 0 & -a_5 & 0 \\ 0 & 0 & 0 & 0 & 0 & 0 & -\delta \end{bmatrix} \quad (10)$$

Using row reduction, $|J - \lambda I| = 0$ we obtained

$$\lambda_1 = -\delta, \; \lambda_2 = -\mu. \quad (11)$$

And the reduced system yields

$$J = \begin{bmatrix} 0 & -a_2 & \sigma & 0 & 0 \\ \frac{-\beta_h\lambda a_2 a_5}{a_7} & 0 & \gamma_2 & \frac{\beta_h(1-A)a_2 a_5 - a_3 a_7}{a_7} & \gamma_1 \\ 0 & 0 & \tau & 0 & -a_4 \\ \varepsilon & 0 & -a_5 & 0 & 0 \\ -(\beta_c\lambda + a_1) & \phi & 0 & \beta_c(1-A) & 0 \end{bmatrix} \quad (12)$$

Letting

$$M = \frac{\beta_h(1-A)a_2 a_5 - a_3 a_7}{a_7}, Q = \frac{\beta_h\lambda a_2 a_5}{a_7}, D = (\beta_c\lambda + a_1), N = \beta_c(1-A),$$

equation (12) becomes:

$$J = \begin{bmatrix} 0 & -a_2 & \sigma & 0 & 0 \\ -Q & 0 & \gamma_2 & M & \gamma_1 \\ 0 & 0 & \tau & 0 & -a_4 \\ \varepsilon & 0 & -a_5 & 0 & 0 \\ -D & \phi & 0 & N & 0 \end{bmatrix} \quad (13)$$

With the characteristics equation of (13) yielding

$$\lambda^5 - \tau\lambda^4 - (\varphi\gamma_1 + Qa_2)\lambda^3 - \begin{pmatrix} Da_2\gamma_1 - D\sigma a_4 + \\ \varphi\gamma_2 a_4 - Na_5 a_4 - \varphi\gamma_1\tau \\ -\varepsilon a_2 M - \tau Q a_2 \end{pmatrix}\lambda^2 - \begin{pmatrix} Da_2\gamma_2 a_4 - \varphi Q\sigma a_4 - \varphi M a_5 a_4 - \\ N\varepsilon a_2\gamma_1 + N\varepsilon\sigma a_4 - \\ \tau Da_2\gamma_1 + \varepsilon a_2 M\tau \end{pmatrix}\lambda + N\varepsilon a_2\gamma_2 a_4 -$$
$$\varphi M\varepsilon\sigma a_4 - Qa_2 Na_5 a_4 - \tau N\varepsilon a_2\gamma_1 = 0 \quad (14)$$

From (14), there is a consistent distribution of negative signs in the characteristic equation. Following Descartes' rule of signs, it is assured that the polynomial has only negative roots. Therefore, all eigenvalues are negative and the system is locally stable. Hence, the proof is complete.

### 2.3.4. Basic Reproduction Number $R_0$

The basic reproduction number measures transmission potential, with values above one indicating spread and below one indicating control. Mathematically, $R_e = \rho(K)$ where $\rho$ is the maximum absolute value of the eigenvalues of matrix $K = FxV^{-1}$. Now consider the transition matrices given by:

$$f = \begin{pmatrix} \beta_h\lambda S(1-A) & 0 & 0 \\ 0 & 0 & 0 \\ 0 & 0 & 0 \end{pmatrix} V = \begin{pmatrix} -a_3 & 0 & 0 \\ \gamma_1 & -a_4 & 0 \\ \theta & 0 & -\delta \end{pmatrix} \quad (15)$$

Now,

$$K = fV^{-1} = \begin{pmatrix} \frac{\beta_h S\lambda(1-A)}{a_3} & 0 & 0 \\ 0 & 0 & 0 \\ 0 & 0 & 0 \end{pmatrix} \quad (16)$$

With spectral radius of:

$$R_0 = \rho(K) = \frac{\beta_h\lambda(1-A)}{a_3}S. \quad (17)$$

Substituting the value of $a_3$ in (17) at disease free value of $S = S_0$:

$$R_0 = \frac{\Lambda\beta_h\lambda(1-A)(\sigma+\mu)(\varepsilon+\mu)}{(\gamma_1+\gamma_2+d_1+\mu)((\sigma+\mu)(\varepsilon+\mu)(\mu+\varphi\eta) - \varepsilon\delta\varphi)} \quad (18)$$

**Table 2:** Variables, parameters, and their corresponding values.

| Variables | Value |
|---|---|
| $m_1$ | 9000 |

| | |
|---|---|
| $m_2$ | 3000 |
| $m_3$ | 7000 |
| $m_4$ | 5000 |
| $m_5$ | 4000 |
| $m_6$ | 1500 |
| $m_7$ | 2000 |
| **Parameters** | |
| $\Lambda$ | 15.1854 |
| $\beta_h$ | 0.0040963 |
| $\beta_c$ | 0.2143 |
| $A$ | $0 \le A \le 1$, 0.39 |
| $\sigma$ | 0.5 |
| $\mu$ | 1/60 |
| $\varepsilon$ | 0.01 |
| $\gamma_1$ | 0.00331423 |
| $\gamma_2$ | 0.1 |
| $d_1$ | 0.09 |
| $d_2$ | 0.05 |
| $\phi$ | 0.07 |
| $\eta$ | 0.7 |
| $\delta$ | 0.83 |
| $\theta$ | 10 |
| $\lambda$ | 0.07 |
| $\tau$ | 0.1 |

**2.3.5. Sensitivity of reproductive number.**

Evaluate $R_0$, using the normalised sensitivity index $S_{\mathrm{K}}^{\Re_e} = \frac{\partial \Re_e}{\partial \mathrm{K}} \cdot \frac{\mathrm{K}}{\Re_e}$. The numerical values are presented in Table 3.

**Table 3:** Sensitivity of model parameters on $R_0$

| Parameters | Sensitivity indices |
|---|---|
| $\Lambda$ | 1 |
| $\beta_h$ | 1 |
| $A$ | -0.6393442623 |
| $\sigma$ | -4.612127286 |
| $\mu$ | -0.2739482871 |
| $\varepsilon$ | 0.0006673950224 |
| $\gamma_1$ | -0.00001988528456 |
| $\gamma_2$ | -0.5999880686 |
| $d_1$ | -0.2999940343 |
| $\phi$ | -0.9804546948 |
| $\eta$ | -5.746319557 |
| $\delta$ | -4.765864863 |

Following the sensitivity results data presented on Table 2, negative parameters help control; positive ones require close monitoring.

## 3. THE FRACTIONAL ORDER MODEL

Fractional-order CF-derivative $\alpha \in (0,1]$ cholera system with memory effects in vaccination analyzed. The right-hand sides of the classical model (7) is of $time^{-1}$, therefore, the proposed fractional order model is of $time^{-\alpha}$.For dimensional consistency, all nonnegative parameters are raised to a fractional order power of $\alpha \in (0,1]$ and this leads to equation (19) to (25):

$$ {}_0^{CF}D^{\alpha}S(t) = \Lambda^{\alpha} - \left(\beta_c{}^{\alpha}\lambda^{\alpha} + \beta_h{}^{\alpha}I(t)\right)S(t) - \left(\mu^{\alpha} + \varphi^{\alpha} + \eta^{\alpha}\right)S(t) + \varepsilon^{\alpha}R(t) \quad (19)$$

$$ {}_0^{CF}D^{\alpha}V(t) = \varphi^{\alpha}S(t) - (\sigma^{\alpha} + \mu^{\alpha})V(t) \quad (20)$$

$$ {}_0^{CF}D^{\alpha}P(t) = A^{\alpha}S(t)\left(\beta_c{}^{\alpha}\lambda^{\alpha} + \beta_h{}^{\alpha}I(t)\right) + \eta^{\alpha}S(t) - \mu^{\alpha}P(t) \quad (21)$$

$$ {}_0^{CF}D^{\alpha}I(t) = \left(\beta_c{}^{\alpha}\lambda^{\alpha} + \beta_h{}^{\alpha}I(t)\right)\left(1 - A^{\alpha}\right)S(t) - \left(\gamma_1{}^{\alpha} + \gamma_2{}^{\alpha} + d_1{}^{\alpha} + \mu^{\alpha}\right)I(t) \quad (22)$$

$$ {}_0^{CF}D^{\alpha}H(t) = \gamma_1{}^{\alpha}I(t) - \left(\tau^{\alpha} + d_2{}^{\alpha} + \mu^{\alpha}\right)H(t) \quad (23)$$

$$ {}_0^{CF}D^{\alpha}R(t) = \sigma^{\alpha}V(t) + \tau^{\alpha}H(t) + \gamma_2{}^{\alpha}I(t) - \varepsilon^{\alpha}R(t) - \mu^{\alpha}R(t) \quad (24)$$

$$ {}_0^{CF}D^{\alpha}B(t) = \theta^{\alpha}I(t) - \delta^{\alpha}B(t) \quad (25)$$

### 3.1. Existence and Uniqueness Analysis

In this section, we apply the fixed-point theory approach to ensure the existence and uniqueness of the fractional order model. Thus, rewriting equation (19) to (25) in their functional form we have

$$\left.\begin{array}{l} {}_0^{CF}D_t^{\alpha}S(t) = K_1(t,S(t)),\ {}_0^{CF}D_t^{\alpha}V(t) = K_2(t,V(t)), \\ {}_0^{CF}D_t^{\alpha}P(t) = K_3(t,P(t)),\ {}_0^{CF}D_t^{\alpha}I(t) = K_4(t,I(t)), \\ {}_0^{CF}D_t^{\alpha}H(t) = K_5(t,H(t)),\quad {}_0^{CF}D_t^{\alpha}R(t) = K_6(t,R(t)), \\ {}_0^{CF}D_t^{\alpha}B(t) = K_7(t,B(t)). \end{array}\right\} \quad (25)$$

Applying Definition 2, the integral operator can be applied on both sides of (25).

**Theorem 2:**

The Lipchitz criterion of contraction is satisfied by kernel $K_1$ this inequality hold;

$$0 \le \left(\beta_c{}^{\alpha}\lambda^{\alpha} + \beta_h{}^{\alpha}\|I\| + \mu^{\alpha} + \phi^{\alpha} + \eta^{\alpha}\right) < 1.$$

**Proof:**

$$\left\|K_1(t,S_1)-K_1(t,S_2)\right\|=\left\|\begin{bmatrix}\left[\beta_c{}^{\alpha}\lambda^{\alpha}+\beta_h^{\alpha}\|I\|\right]\\ \left[S_1(t)-S_2(t)\right]\end{bmatrix}-\begin{bmatrix}\left[\mu^{\alpha}+\varphi^{\alpha}+\eta^{\alpha}\right]\\ \left[S_1(t)-S_2(t)\right]\end{bmatrix}\right\|$$

$$\le\left\|\beta_c{}^{\alpha}\lambda^{\alpha}+\beta_h^{\alpha}\|I\|\right\|\left\|S_1(t)-S_2(t)\right\|+\left\|\mu^{\alpha}+\varphi^{\alpha}+\eta^{\alpha}\right\|$$

$$\left\|S_1(t)-S_2(t)\right\|\le\left\|S_1(t)-S_2(t)\right\|\beta_c{}^{\alpha}\lambda^{\alpha}+\beta_h^{\alpha}\|I\|+\left(\mu^{\alpha}+\varphi^{\alpha}+\eta^{\alpha}\right)\Big\|.$$

Let $K_1=\left\|\beta_c{}^{\alpha}\lambda^{\alpha}+\beta_h^{\alpha}\|I\|+\left(\mu^{\alpha}+\phi^{\alpha}+\eta^{\alpha}\right)\right\|$,

and $\|I\|\le\delta_{\psi}$, is bounded such that

$$\left\|K_1(t,S)-K_1(t,S_1)\right\|\le L_1\left\|S_1(t)-S_2(t)\right\|$$

Then the Lipchitz condition is satisfied for $K_1$, $0\le\left(\beta_c{}^{\alpha}\lambda^{\alpha}+\beta_h{}^{\alpha}\|I\|+\mu^{\alpha}+\phi^{\alpha}+\eta^{\alpha}\right)<1$ and $K_1$ contracts.

Similar to the Lipchitz condition of other functionals and a contraction occurs for each when

$$L_2=0\le\mu^{\alpha}+\sigma^{\alpha}<1,\qquad L_3=0\le\mu^{\alpha}<1,$$

$$L_4=0\le\begin{pmatrix}\beta_c{}^{\alpha}\lambda^{\alpha}+\beta_h{}^{\alpha}\delta^{\alpha}{}_{\psi}+\mu^{\alpha}+\varphi^{\alpha}+\eta^{\alpha}\\ +\gamma_1{}^{\alpha}+\gamma_2^{\alpha}+d_1^{\alpha}+\mu^{\alpha}\end{pmatrix}<1$$

, $L_5=0\le\tau^{\alpha}+d_2^{\alpha}+\mu^{\alpha}<1,$

$L_6=0\le\varepsilon^{\alpha}+\mu^{\alpha}<1, L_7=0\le\delta^{\alpha}<1.$

Furthermore consider the following recursive form given by:

$$G_{1n}(t)=S_n(t)-S_{n-1}(t)\frac{2(1-\alpha)}{(2-\alpha)N(\alpha)}\begin{bmatrix}K_1(t,S_{n-1})\\ -K_1(t,S_{n-2})\end{bmatrix}+\frac{2\alpha}{(2-\alpha)N(\alpha)}\int_0^t K_1(\alpha,S_{n-1})d\alpha$$

$$G_{2n}(t)=V_n(t)-V_{n-1}(t)\frac{2(1-\alpha)}{(2-\alpha)N(\alpha)}\begin{bmatrix}K_2(t,V_{n-1})\\ -K_2(t,V_{n-2})\end{bmatrix}+\frac{2\alpha}{(2-\alpha)N(\alpha)}\int_0^t K_2(\alpha,V_{n-1})d\alpha$$

$$G_{3n}(t)=P_n(t)-P_{n-1}(t)\frac{2(1-\alpha)}{(2-\alpha)N(\alpha)}\begin{bmatrix}K_3(t,P_{n-1})\\ -K_3(t,P_{n-2})\end{bmatrix}+\frac{2\alpha}{(2-\alpha)N(\alpha)}\int_0^t K_3(\alpha,P_{n-1})d\alpha$$

$$G_{4n}(t)=I_n(t)-I_{n-1}(t)\frac{2(1-\alpha)}{(2-\alpha)N(\alpha)}\begin{bmatrix}K_4(t,I_{n-1})\\ -K_4(t,I_{n-2})\end{bmatrix}+\frac{2\alpha}{(2-\alpha)N(\alpha)}\int_0^t K_4(\alpha,I_{n-1})d\alpha$$

$$G_{5n}(t)=H_n(t)-H_{n-1}(t)\frac{2(1-\alpha)}{(2-\alpha)N(\alpha)}\begin{bmatrix}K_5(t,H_{n-1})\\ -K_5(t,H_{n-2})\end{bmatrix}+\frac{2\alpha}{(2-\alpha)N(\alpha)}\int_0^t K_5(\alpha,H_{n-1})d\alpha$$

$$G_{6n}(t)=R_n(t)-R_{n-1}(t)\frac{2(1-\alpha)}{(2-\alpha)N(\alpha)}\begin{bmatrix}K_6(t,R_{n-1})\\ -K_6(t_1,R_{n-2})\end{bmatrix}+\frac{2\alpha}{(2-\alpha)N(\alpha)}\int_0^t K_6(\alpha,R_{n-1})d\alpha$$

$$G_{7n}(t)=B_n(t)-B_{n-1}(t)\frac{2(1-\alpha)}{(2-\alpha)N(\alpha)}\begin{bmatrix}K_7(t,B_{n-1})\\ -K_7(t,B_{n-2})\end{bmatrix}+\frac{2\alpha}{(2-\alpha)N(\alpha)}\int_0^t K_7(\alpha,B_{n-1})d\alpha$$

Subject to conditions:

$S_0(t)=m_1, V_0(t)=m_2, P_0(t)=m_3,$

$I_0(t)=m_4, H_0(t)=m_5, R_0(t)=m_6,$ .

$B_0(t)=m_7.$

Taking the norm of the above equations and applying the Lipchitz condition

$$\left\|G_{1n}(t)\right\|\le\frac{2(1-\alpha)}{(2-\alpha)N(\alpha)}L_1\left\|G_{1(n-1)}(t)\right\|+\frac{2\alpha}{(2-\alpha)N(\alpha)}L_1\times\int_0^t\left\|G_{1(n-1)}(\alpha)\right\|d\alpha,$$

$$\left\|G_{2n}(t)\right\|\le\frac{2(1-\alpha)}{(2-\alpha)N(\alpha)}L_2\left\|G_{2(n-1)}(t)\right\|+\frac{2\alpha}{(2-\alpha)N(\alpha)}L_2\times\int_0^t\left\|G_{2(n-1)}(\alpha)\right\|d\alpha.$$

In general,

$$\left\|G_{in}(t)\right\|\le\frac{2(1-\alpha)}{(2-\alpha)N(\alpha)}L_i\left\|G_{i(n-1)}(t)\right\|+\frac{2\alpha}{(2-\alpha)N(\alpha)}L_i\times\int_0^t\left\|G_{i(n-1)}(\alpha)\right\|d\alpha,$$

$j=3..8$

So that

$$S_n(t)=\sum_{n=1}^{j}G_{1n}(t),V_n(t)=\sum_{n=1}^{j}G_{2n}(t),P_n(t)$$
$$=\sum_{n=1}^{j}G_{3n}(t),I_n(t)=\sum_{n=1}^{j}G_{4n}(t),$$
$$H_n(t)=\sum_{n=1}^{j}G_{5n}(t),\ R_n(t)=\sum_{n=1}^{j}G_{6n}(t),$$
$$B_n(t)=\sum_{n=1}^{j}G_{7n}(t).$$

This complete the proof. Thus, a unique and continuous solution exists for the system.

### 3.2. Model solution using the LADM

Adapting the generalised methodology in section 2 to the fractional order mode,by definition, $\ell\left[{}_0^{CF}D^{\alpha}f(t)\right]=\dfrac{s\ell\left(f(t)-f(0)\right)}{s+\alpha(1-s)}$ for $0<\alpha\le 1$.

Then simplifying and taking the inverse Laplace transform of both sides yields:

$$S(t)=\ell^{-1}\left(\frac{S(0)}{s}\right)+\ell^{-1}\left(\begin{array}{l}\dfrac{s+\alpha(1-s)}{s}\\ \ell\left[\begin{array}{l}\Lambda^{\alpha}-\left(\beta_c{}^{\alpha}\lambda^{\alpha}+\beta_h{}^{\alpha}I(t)\right)S(t)-\\ \left(\mu^{\alpha}+\varphi^{\alpha}+\eta^{\alpha}\right)S(t)+\varepsilon^{\alpha}R(t)\end{array}\right]\end{array}\right)$$

(26)

$$V(t)=\ell^{-1}\left(\frac{V_1(0)}{s}\right)+\ell^{-1}\left(\begin{array}{l}\dfrac{s+\alpha(1-s)}{s}\\ \ell\left[\varphi^{\alpha}S(t)-(\sigma^{\alpha}+\mu^{\alpha})V(t)\right]\end{array}\right)$$

(27)

$$P(t)=\ell^{-1}\left(\frac{P(0)}{s}\right)+\ell^{-1}\left(\begin{array}{l}\dfrac{s+\alpha(1-s)}{s}\\ \ell\left[\begin{array}{l}A^{\alpha}S(t)\left(\beta_c{}^{\alpha}\lambda^{\alpha}+\beta_h{}^{\alpha}I(t)\right)\\ +\eta^{\alpha}S(t)-\mu^{\alpha}P(t)\end{array}\right]\end{array}\right)$$

(28)

$$I(t)=\ell^{-1}\left(\frac{I(0)}{s}\right)+\ell^{-1}\left(\begin{array}{l}\dfrac{s+\alpha(1-s)}{s}\\ \ell\left[\begin{array}{l}\left(\beta_c{}^{\alpha}\lambda^{\alpha}+\beta_h{}^{\alpha}I(t)\right)\left(1-A^{\alpha}\right)\\ S(t)-\left(\gamma_1{}^{\alpha}+\gamma_2{}^{\alpha}+d_1{}^{\alpha}+\mu^{\alpha}\right)I(t)\end{array}\right]\end{array}\right)$$

(29)

$$H(t)=\ell^{-1}\left(\frac{H(0)}{s}\right)+\ell^{-1}\left(\begin{array}{l}\dfrac{s+\alpha(1-s)}{s}\\ \ell\left[\gamma_1{}^{\alpha}I(t)-\left(\tau^{\alpha}+d_2{}^{\alpha}+\mu^{\alpha}\right)H(t)\right]\end{array}\right)$$

(30)

$$R(t)=\ell^{-1}\left(\frac{R(0)}{s}\right)+\ell^{-1}\left(\begin{array}{l}\dfrac{s+\alpha(1-s)}{s}\ell\left[\begin{array}{l}\sigma^{\alpha}V(t)+\tau^{\alpha}H(t)\\ +\gamma_2{}^{\alpha}I(t)-\\ \varepsilon^{\alpha}R(t)-\mu^{\alpha}R(t)\end{array}\right]\end{array}\right)$$

(31)

$$B(t)=\ell^{-1}\left(\frac{B(0)}{s}\right)+\ell^{-1}\left(\frac{s+\alpha(1-s)}{s}\ell\left[\theta^{\alpha}I(t)-\delta^{\alpha}B(t)\right]\right).$$

(32)

Representing the model variables as infinite sum of their partial sequence, the nonlinear team:

$$\sum_{m=0}^{\infty}Q_m(t)=S(t)I(t). \tag{33}$$

Using the Adomian Polynomial given by:

$$Q_n(t)=\frac{1}{\Gamma(m+1)}\frac{d}{d\chi^m}\left[\sum_{j=0}^{m}\chi^j S_j(t)\sum_{j=0}^{m}\chi^j I_j(t)\right]_{\xi=0}\Bigg\}$$

(34)

Evaluating (26) to (32) with (33) and (34). Subsequent utility of the initial conditions $S(0)=m_1,\ V(0)=m_2,\ P(0)=m_3,\ I(0)=m_4,$ $H(0)=m_5, R(0)=m_6,\ B(0)=m_7$ such that first approximation yields:

$S_0(t)=m_1,\ V_0(t)=m_2,\ P_0(t)=m_3,$
$I_0(t)=m_4,\ H_0(t)=m_5, R_0(t)=m_6,\ B_0(t)=m_7.$

Evaluating at n=0 and the first approximate results are obtained as:

$$S_1(t)=(\alpha(t-1)+1)\left(\begin{array}{l}\Lambda^{\alpha}+\varepsilon^{\alpha}m_6-\\ m_1\left(\beta_c{}^{\alpha}\lambda^{\alpha}+\eta^{\alpha}+\phi^{\alpha}+\mu^{\alpha}+\beta_h{}^{\alpha}m_4\right)\end{array}\right),$$
$$V_1(t)=(\alpha(t-1)+1)\left(\phi^{\alpha}m_1-\sigma^{\alpha}m_2-\mu^{\alpha}m_2\right),$$
$$P_1(t)=(\alpha(t-1)+1)\left(\begin{array}{l}A^{\alpha}m_1\beta_c{}^{\alpha}\lambda^{\alpha}+A^{\alpha}m_1\beta_h{}^{\alpha}m_4\\ +\eta^{\alpha}m_1-\mu^{\alpha}m_3\end{array}\right),$$
$$I_1(t)=(\alpha(t-1)+1)\left(\begin{array}{l}\left(\begin{array}{l}m_1\beta_h{}^{\alpha}-\mu^{\alpha}-d_1{}^{\alpha}-\gamma_2{}^{\alpha}\\ -\gamma_1{}^{\alpha}-m_1A^{\alpha}\beta_h{}^{\alpha}\end{array}\right)m_4\\ +\beta_c{}^{\alpha}\left(1-A^{\alpha}\right)\lambda^{\alpha}m_1\end{array}\right),$$
$$H_1(t)=(\alpha(t-1)+1)\left(\gamma_1{}^{\alpha}m_4-\left(\tau^{\alpha}+d_2{}^{\alpha}+\mu^{\alpha}\right)m_5\right),$$
$$R_1(t)=(\alpha(t-1)+1)\left(\sigma^{\alpha}m_4+\tau^{\alpha}m_5+\gamma_2{}^{\alpha}m_4-\varepsilon^{\alpha}m_6-\mu^{\alpha}m_6\right),$$
$$B(t)=(\alpha(t-1)+1)\left(\theta^{\alpha}m_4-\delta^{\alpha}m_7\right).$$

Following the same process, additional iterations are computed and the model solution to third approximation in this study is:

$$\left.\begin{aligned} S(t)=\sum_{m=0}^{3}S_m(t), V(t)=\sum_{m=0}^{3}V_m(t), \\ P(t)=\sum_{m=0}^{3}P_n(t), I(t)=\sum_{m=0}^{3}I_m(t), \\ H(t)=\sum_{m=0}^{3}H_m(t), R(t)=\sum_{m=0}^{3}R_m(t), B(t)=\sum_{m=0}^{3}B_m(t). \end{aligned}\right\} \quad (36)$$

### 3.3. Convergence Analysis

We infer to ref. [17] to demonstrate the convergence of solution. The iterative solution (36) is illustrated as $v_n=\Omega v_{n-1}$, $v_{n-1}=\sum_{j=1}^{n}v_j \quad n=1,2,3,...,$ we prove the convergence of $\{v_n\}$, using the subsequent theorem.

**Theorem 3:**

Let $B_1$ be a Banach Space and $\Omega: B_1 \to B_1$ a contraction functions with constant $0<\delta<1$, then there exist a unique point $\upsilon$ in $\Omega$ such that $\Omega(\upsilon)=\upsilon$ and $\upsilon=(S,V,P,I,H,R,B)$. Let $\upsilon_0=\upsilon_0\in P_s(w)$, where $P_s(\upsilon)=\{\upsilon'\in B_1 : \|\upsilon'-\upsilon\|<s\}$ then, we have $\upsilon_m\in P_s(\upsilon)\ \forall\ m$ and $\upsilon_m\to\upsilon$.

**Proof:**

Using mathematical induction, when $m=1$, $\|\upsilon_0-\upsilon\|=\|\Omega(\upsilon_0)-\Omega(\upsilon)\|\le\delta\|\upsilon_0-\upsilon\|$. If at $m=1$, the problem is true, then $\|\upsilon_{m-1}-\upsilon\|\le\delta^{m-1}\|\upsilon_0-\upsilon\|$ so that $\|\upsilon_n-\upsilon\|=\|\Omega(\upsilon_{n-1})-\Omega(\upsilon)\|\le\delta\|\upsilon_{m-1}-\upsilon\|\le\delta^m\|\upsilon_0-\upsilon\|$. Again, $\upsilon_0\in P_s(\upsilon)$ by implication, $\|\upsilon_0-\upsilon\|<s$ and $\|\upsilon_n-\upsilon\|\le\delta^m\|\upsilon_0-\upsilon\|\le\delta^m s<s$.

Consequently, this proves that $\upsilon_m\in P_s(\upsilon)$. Moreover, since $\lim_{m\to\infty}\delta^m=0$ therefore, $\lim_{m\to\infty}\delta^m\|\upsilon_n-\upsilon\|=0$ and $\lim_{m\to\infty}\upsilon_m=\upsilon$ which completes the proof.

## 4. RESULTS

This section presents basic information about the analysis, performed using Maple 13 software. Due to limited data availability, compartment and parameter values were assumed. Table 2 summarizes these variables, parameters, and their values.

## 5. NUMERICAL SIMULATIONS

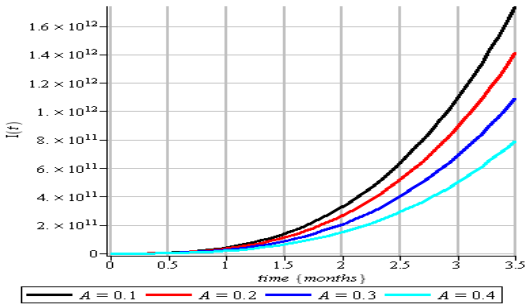


**Fig.1:** Dynamic impact of high-risk population's adoption of protective measures on infected population.

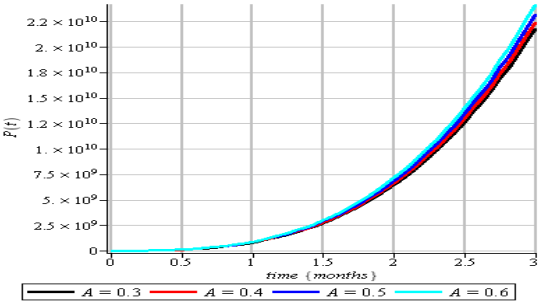


**Fig.2:** Dynamic impact of high-risk population's adoption of protective measures on protected population.

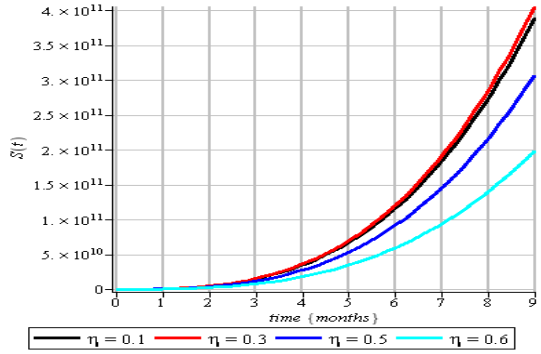


**Fig. 3:** Dynamics of susceptible people to adoptance rate of protective measures

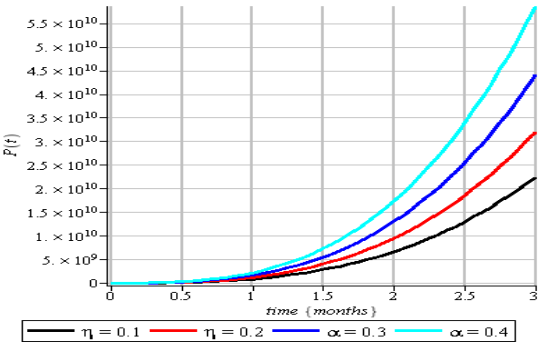


**Fig. 4:** Dynamics of protected people to adoptance rate of protective measures

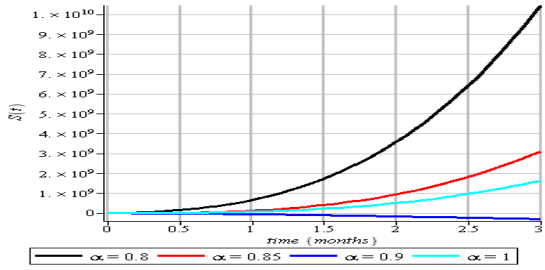


**Fig. 5:** Dynamic response of susceptible people to the fractional order rate of eradication factors.

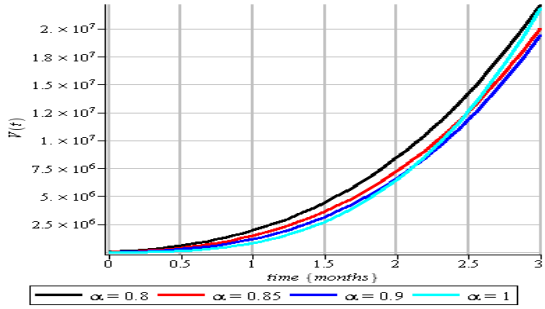


**Fig. 6:** Dynamic response of vaccinated people to the fractional order rate of eradication factors

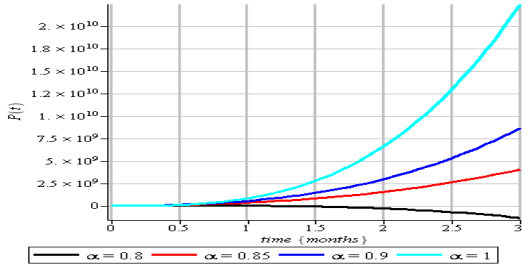


**Fig. 7:** Dynamic response of protected people to the fractional order rate of eradication factors

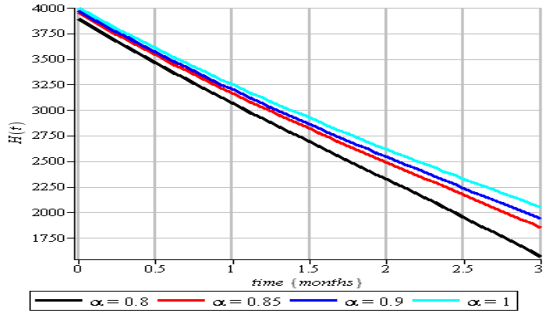


**Fig. 8:** Dynamic response of hospitalized people to the fractional order rate of eradication factors

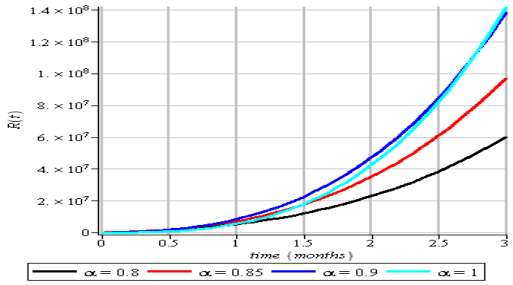


**Fig. 9:** Dynamic response of model variables to the fractional order rate of eradication factors,

## 6. DISCUSSION

This section discusses the study results. Fig. 1 shows a significant decrease in the population of infected individuals as the adoption rate of preventive measures increases among susceptible individuals in high-risk regions. Conversely, Fig. 2 demonstrates a notable increase in the population of protected individuals corresponding to higher rates of protective measures. Results shown in Figs 3 and 4 demonstrate the dynamic response of the susceptible and protected populations to variations in the protection rate. Specifically, Fig. 3 illustrates a significant decrease in the population of susceptible individuals, indicating heightened protection against the targeted threat. Conversely, Fig. 4 reveals a substantial increase in the population of protected individuals, demonstrating the effectiveness of the implemented protective measures in shielding the population from harm.

Figs 5-9 present the significant effects of changes in the fractional order level of intervention rates on population variables. In Fig. 5, increasing the fractional order level of intervention rate, particularly in protective measures, leads to a higher level of awareness and knowledge about disease prevention among the population, thereby reducing the number of susceptible individuals and slowing down the spread of the disease.

On the other hand, Fig. 6 reveals that the protected population increases as the fractional order level of interventions approaches the classical order. This implies that higher rates of awareness of protective measures such as education and vaccination can be applied to achieve herd immunity in the population. Fig. 7 demonstrates that higher rates of adoption of protective measures and vaccination contribute to achieving herd immunity. Figs 8 show a drastic reduction in infected and hospitalized populations as $\alpha$ approaches 1, revealing that high rates of intervention strategies potentially lower the number of infectious individuals. Finally, Fig.9 shows that the recovered population is maximum at integer order, emphasizing the need for maximum implementation of educational awareness of protective measures and vaccination. The overall implication is that vaccination and education are crucial in combating cholera outbreaks. Higher vaccination rates and educational awareness reduce susceptibility, increase protection, and contribute to overall public health resilience against cholera.

## 7. CONCLUSION

This study shows the main strengths of the proposed seven compartment deterministic model that efficiently draws the role of both, vaccination and education in cholera prevention to vulnerable riverine communities, and actual analysis proves that the proportion between the percentage of vaccinated people and level of protection of the population is direct and that the awareness level has an enormous influence on the process of diseases dynamics, where high awareness relates to fewer infections and elevated level of protection. Although its outcomes demonstrate the advantage of using fractional calculus to biological models, such limitations can be mentioned: the deterministic nature could not entirely model randomness of cholera outbreaks, that is based on the assumption of constant behavior patterns, that may be limited in application to certain demographic conditions and that could only be utilized in symbolic computation packages that may not be present or be very inefficient in large-scale or real-time applications. The results present potential application of a public health interventions framework, informing policymakers on how to target specific educational efforts and selectively vaccinate to achieve the most effective herd immunity, healthcare resource development in at-risk populations, as well as emergency response planning, with future studies having the potential to expand this framework by incorporating stochastic modeling to more truly allow the randomness of cholera outbreaks to inform real-world applications.

## REFERENCES


[1]. Amisu BO, Okesanya OJ, Adigun OA, Manirambona E, Ukoaka BM, Lawal OA, Idris NB, Olaleke NO, Okon II, Ogaya JB, Prisno III DE. Cholera resurgence in Africa: assessing progress, challenges, and public health response towards the 2030 global elimination target. Le Infezioni in Medicina. 2024 Jun 1;32(2):148.

[2]. Aborode AT, Adesola RO, Onifade IA, Adesiyan R, Ibiam VA, Jinadu NA, Bakre AA. Outbreak of cholera in Nigeria: the role of One Health. Discover Public Health. 2025 Mar 31;22(1):125.

[3]. Onuorah MO, Atiku FA, Juuko H. Mathematical model for prevention and control of cholera transmission in a variable population. Research in Mathematics. 2022 Dec 31;9(1):2018779.

[4]. Abdul NS, Yahya L, Resmawan R, Nuha AR. Dynamic Analysis of the Mathematical Model of the Spread of Cholera With Vaccination Strategies. BAREKENG J. Ilmu Mat. dan Terap. 2022 Mar 21;16(1):281-92.

[5]. Anteneh LM, Zanvo SD, Traore K, Kakaï RG. Modelling the Impact of Vaccination on Cholera Transmission Dynamics under Stratified Populations and Seasonality. Infectious Disease Modelling. 2025 Jun 23.

[6]. Ratnayake R, Checchi F, Jarvis CI, Edmunds WJ, Finger F. Inference is bliss: simulation for power estimation for an observational study of a cholera outbreak intervention. PLoS neglected tropical diseases. 2022 Feb 16;16(2):e0010163.

[7]. Purohit SD. A novel study of the impact of vaccination on pneumonia via fractional approach. Partial Differential Equations in Applied Mathematics. 2024 Jun 1;10:100698.

[8]. Mustapha UT, Maigoro YA, Yusuf A, Qureshi S. Mathematical modeling for the transmission dynamics of cholera with an optimal control strategy. Bulletin of Biomathematics. 2024;2(1):1-20.

[9]. Cherotich S, Khachiti B, Khakali P, Kendi R. Mathematical Modeling of Cholera Mitigation Incorporating Handwashing. African Scientific Annual Review. 2024 Jun 21;1(Mathematics 1):127-48.

[10]. Anteneh LM, Lokonon BE, Kakaï RG. Modelling techniques in cholera epidemiology: A systematic and critical review. Mathematical Biosciences. 2024 May 20:109210.

[11]. Liouville J. Mémoire sur le calcul des différentielles à indices quelconques. J École Polytech Paris. 1832;13:71–162.

[12]. Alaje AI, Olayiwola MO, Adedokun KA, Adedeji JA, Oladapo AO. Modified homotopy perturbation method and its application to analytical solitons of fractional-order Korteweg–de Vries equation. Beni-Suef University Journal of Basic and Applied Sciences. 2022 Dec 2;11(1):139.

[13]. Olayiwola MO, Oluwafemi EA. Hereditary and Antimicrobial Factor Shaping Extracellular Bacteria Dynamics in an In-Host Mathematical Model of Tuberculosis for Disease Control. Tuberculosis. 2025 Jun 28:102668.

[14]. Caputo M. Elasticità e dissipazione. Bologna: Zanichelli; 1969.

[15]. Adedeji J, Olayiwola MO. ON ANALYSIS OF A MATHEMATICAL MODEL OF CHOLERA USING CAPUTO FRACTIONAL ORDER: ON ANALYSIS OF A MATHEMATICAL MODEL OF CHOLERA. Journal of the Nigerian Mathematical Society. 2024 Sep 26;43(3):287-309.

[16]. Caputo M, Fabrizio M. A new definition of fractional derivative without singular kernel. Progress in Fractional Differentiation & Applications. 2015;1(2):73-85.

[17]. Olayiwola, M.O., Alaje, A.I. Mathematical modelling of diphtheria transmission and vaccine efficacy using Nigeria. Model. Earth Syst. Environ. (2024). https://doi.org/10.1007/s40808-024-01976-7

[18]. Baba IA, Humphries UW, Rihan FA. A well-posed fractional order cholera model with saturated incidence rate. Entropy. 2023 Feb 15;25(2):360.

[19]. Helikumi M, Lolika PO. A note on fractional-order model for cholera disease transmission with control strategies. Commun. Math. Biol. Neurosci.. 2022 Mar 28;2022:Article-ID.

[20]. Rosa S, Torres DF. Fractional-order modelling and optimal control of cholera transmission. Fractal and Fractional. 2021 Dec 7;5(4):261.